



# Androgen Receptor Signalling Promotes a Luminal Phenotype in Mammary Epithelial Cells

Gerard A. Tarulli<sup>1,2</sup> · Geraldine Laven-Law<sup>1</sup> · Mona Shehata<sup>3</sup> · Kirsty A. Walters<sup>4</sup> · Iza M. Denis<sup>1</sup> · Md. Mostafizur Rahman<sup>1</sup> · David J. Handelsman<sup>5</sup> · Nicola R. Dean<sup>6</sup> · Wayne D. Tilley<sup>1</sup> · Theresa E. Hickey<sup>1</sup>

Received: 7 July 2017 / Accepted: 18 July 2018 / Published online: 12 August 2018  
© Springer Science+Business Media, LLC, part of Springer Nature 2018

## Abstract

Androgens influence mammary gland development but the specific role of the androgen receptor (AR) in mammary function is largely unknown. We identified cell subsets that express AR *in vivo* and determined the effect of AR activation and transgenic AR inhibition on sub-populations of the normal mouse mammary epithelium by flow cytometry and immunohistochemistry. Immunolocalisation of AR with markers of lineage identity was also performed in human breast tissues. AR activation *in vivo* significantly decreased the proportion of basal cells, and caused an accumulation of cells that expressed a basal cell marker but exhibited morphological features of luminal identity. Conversely, in AR null mice the proportion of basal mammary epithelial cells was significantly increased. Inhibition of AR increased basal but not luminal progenitor cell activity *in vitro*. A small population of AR-positive cells in a basal-to-luminal phenotype transition was also evident in human breast lobules. Collectively, these data support a role for AR in promoting a luminal phenotype in mammary epithelial cells.

**Keywords** Androgens · Mammary epithelium · Androgen receptor

## Abbreviations

AR	Androgen receptor
DHT	Dihydrotestosterone
ECM	Extracellular matrix
ER	Estrogen receptor-alpha
FACS	Fluorescence-activated cell sorting
HF	Hydroxyflutamide
HS-MEC	Hormone-sensing mammary epithelial cell
MEC	Mammary epithelial cell
PR	Progesterone receptor

## Introduction

The mammary epithelium broadly consists of a single population of basal mammary epithelial cells (MECs) and two populations of luminal MECs: milk producing alveolar MECs that lack estrogen receptor-alpha (ER) and progesterone receptors (PR), as well as ER- and PR-positive hormone-sensing (HS)-MEC. The HS-MECs serve as principal conduits of endocrine reproductive cues, translating these into paracrine signals for proliferation and differentiation in nearby MECs (reviewed in [1]). Turnover of the mammary

**Electronic supplementary material** The online version of this article (<https://doi.org/10.1007/s10911-018-9406-2>) contains supplementary material, which is available to authorized users.

✉ Gerard A. Tarulli  
gerard.tarulli@unimelb.edu.au

✉ Theresa E. Hickey  
theresa.hickey@adelaide.edu.au

<sup>1</sup> Dame Roma Mitchell Cancer Research Laboratories, Faculty of Health & Medical Sciences, The University of Adelaide, Adelaide, SA 5005, Australia

<sup>2</sup> School of BioSciences, The University of Melbourne, Parkville, Victoria 3052, Australia

<sup>3</sup> Princess Margaret Cancer Centre, University Health Network, Toronto, Ontario M5G 1L7, Canada

<sup>4</sup> Discipline of Obstetrics & Gynaecology, School of Women's & Children's Health, University of New South Wales, Sydney, New South Wales 2052, Australia

<sup>5</sup> Andrology Laboratory, ANZAC Research Institute, University of Sydney, Sydney, New South Wales 2139, Australia

<sup>6</sup> Department of Plastic & Reconstructive Surgery, Flinders Medical Centre/Flinders University, Bedford Park, SA 5042, Australia

epithelium is thought to be undertaken by stem/bipotent progenitors that can differentiate into either basal or luminal MECs [2], as well as a population of basal- or luminal-restricted progenitors [3, 4].

Although estrogen and progesterone drive mammary development, androgen hormones are also found in physiological concentrations in the circulation of women. The receptor for androgens, the androgen receptor (AR), is expressed in diverse tissues including normal breast. Androgens have long been known to inhibit breast growth in pubertal boys [5], and are a major contributor to the inhibition of breast growth in pubertal girls with congenital adrenal hyperplasia characterised by normal levels of estrogens in the presence of relatively high androgen levels [6]. Together, this has led to the idea that androgens act to inhibit the activity of estrogen in the mammary epithelium, specifically within the cells responding directly to estrogenic hormones, namely the HS-MEC population. This notion is supported by findings of a high degree of cellular co-expression for AR and ER in normal human and primate mammary epithelium, as well as in breast cancers (reviewed in [7, 8]), the inhibition of mammary outgrowth by androgen treatment of pubertal mice [9], as well as the acceleration of mammary development through puberty in the AR-null mouse [10]. It is also well known that breast cancers may express AR in the absence of ER (reviewed in [7, 11]). This may reflect an unknown action for the AR in populations outside ER-positive HS-MECs of normal mammary epithelium.

This study aimed to determine which cells within the mammary epithelium have the capacity to respond directly to androgen hormones, and the consequence of AR modulation on differentiation of MEC sub-populations. We demonstrate the presence of high AR levels in the HS-MEC population, reveal AR expression in basal MECs, and through molecular activation or transgenic AR inhibition, uncover a novel role for AR in promoting luminal identity in normal MECs.

## Results

### AR Activation Inhibits Mammary Ductal Side-Branching and Modifies Epithelial Content in Adult Mice

A non-steroidal androgen currently in clinical trials for breast cancer (GTx-024; Enobosarm®, [12]; NCT02971761, NCT01616758, NCT02463032) was employed for in vivo studies to avoid metabolism of androgens into estrogenic or progestogenic ligands. Carmine-stained whole mount analysis was used to assess mammary ductal branching (Fig. 1A). Normal ductal side-branching was evident in vehicle-treated mice, and mice treated with GTx-024 at low (0.1 mg/kg/day)

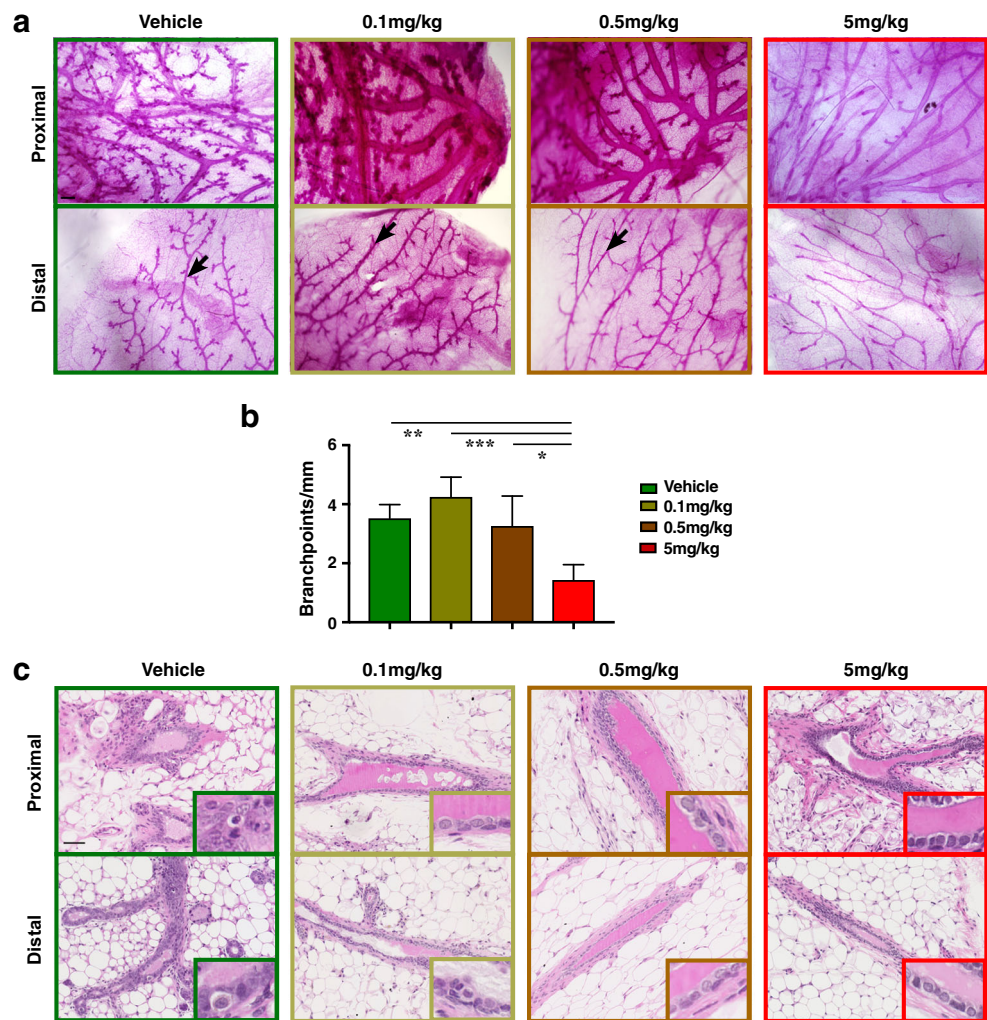
and intermediate (0.5 mg/kg/day) doses. In contrast, high dose GTx-024 (5 mg/kg/day) reduced side-branching by approximately 50% (quantification in Fig. 1B), a result consistent with a previous finding in the adult mouse using the AR activator, dihydrotestosterone (DHT) [9]. At a histological level, treatment of mice with any dose of GTx-024 did not result in gross changes in mammary histology, though apparent reductions in cytoplasmic staining density were observed (Fig. 1C).

### AR Activation Increases the Proportion of Luminal MECs In Vivo

To determine whether AR activation alters the balance of MEC sub-populations, mouse mammary glands from vehicle- and GTx-024-treated mice were digested, immunolabeled and assessed by flow cytometry. At the highest dose of GTx-024 (5 mg/kg/day) the proportion of total epithelial cells was reduced by 50% (example flow cytometry plots in Fig. 2A, with quantification in Fig. 2B,  $p < 0.001$ ), while the proportion of total epithelial cells was remarkably consistent between vehicle and mice receiving low (0.1 mg/kg/day) or intermediate (0.5 mg/kg/day) doses. The proportion of luminal cells was significantly increased at both intermediate and high doses ( $p < 0.01$ ) while no change was observed at the low dose of GTx-024. No alterations in the proportion of luminal sub-populations (alveolar or HS-MEC) were observed (Supplemental Fig. S1). These findings indicate that AR activation in vivo exerted two principle effects on MECs: a reduction in total MECs at a high dose and an increase in the proportion of luminal MECs at intermediate and high doses, when assessed by flow cytometry.

To more directly assess how AR activation alters the balance of MEC sub-populations in situ, we examined the expression of MEC lineage markers by immunohistochemistry (IHC). In vehicle-treated mice, the basal marker p63 [13, 14] is expressed in basally orientated and positioned MECs (Fig. 2C, green boxes, arrow), while in mice treated with GTx-024 at 0.5 mg/kg, p63-expressing MECs were found in a luminal position and possessing luminal morphology (Fig. 2C, brown boxes, arrowheads, with quantification of basal MEC proportions in C'). The proportion of p63-expressing cells in a luminal position was  $0.02\% \pm 0.01\%$  vs.  $0.59\% \pm 0.19\%$  for vehicle and 0.5 mg/kg/day GTx-024, respectively ( $p < 0.04$ ). There was also a significant reduction in the relative proportion of p63-expressing MECs in all treatment groups (Fig. 2C',  $p < 0.002$ ). The HS-MEC population is defined by expression of ER (Fig. 2D), detectable in a subset of luminal MECs. A significant increase in the proportion of ER-positive cells was identified in mice treated with 5 mg/kg/day and 0.5 mg/kg/day of GTx-024 (Fig. 2D',  $p < 0.01$ ). The proportion of MECs expressing the luminal alveolar marker Elf5 [15] was reduced in mice treated with GTx-024 only at the 0.5 mg/kg/day dose (Fig. 2E, with quantification in E',  $p <$

**Fig. 1** AR activation inhibits mouse mammary ductal side-branching. **a)** Carmine-stained thoracic mammary whole-mounts from mice treated for 16 weeks with vehicle, 0.1, 0.5 or 5 mg/kg/day GTx-024, representing the proximal (upper panels) and distal (lower panels) regions of the ductal tree. Side branches indicated by arrows (scale bar = 200  $\mu$ m). **b)** Quantification of ductal side-branching in A ( $n = 5$  animals/group, mean  $\pm$  s.d.). **c)** Haematoxylin and eosin-stained mammary tissue sections, depicting large ducts (proximal - upper panels) and smaller ducts (distal - lower panels). ( $n = 5$  mice/group, scale bar = 50  $\mu$ m)



0.03), and this change was modest compared with changes in basal and HS-MEC, suggesting these latter cell types as the principal populations modified by AR activation. These results demonstrate that activation of the AR in vivo results in accumulation of ER+ luminal MECs with a concordant reduction in the p63-expressing basal population.

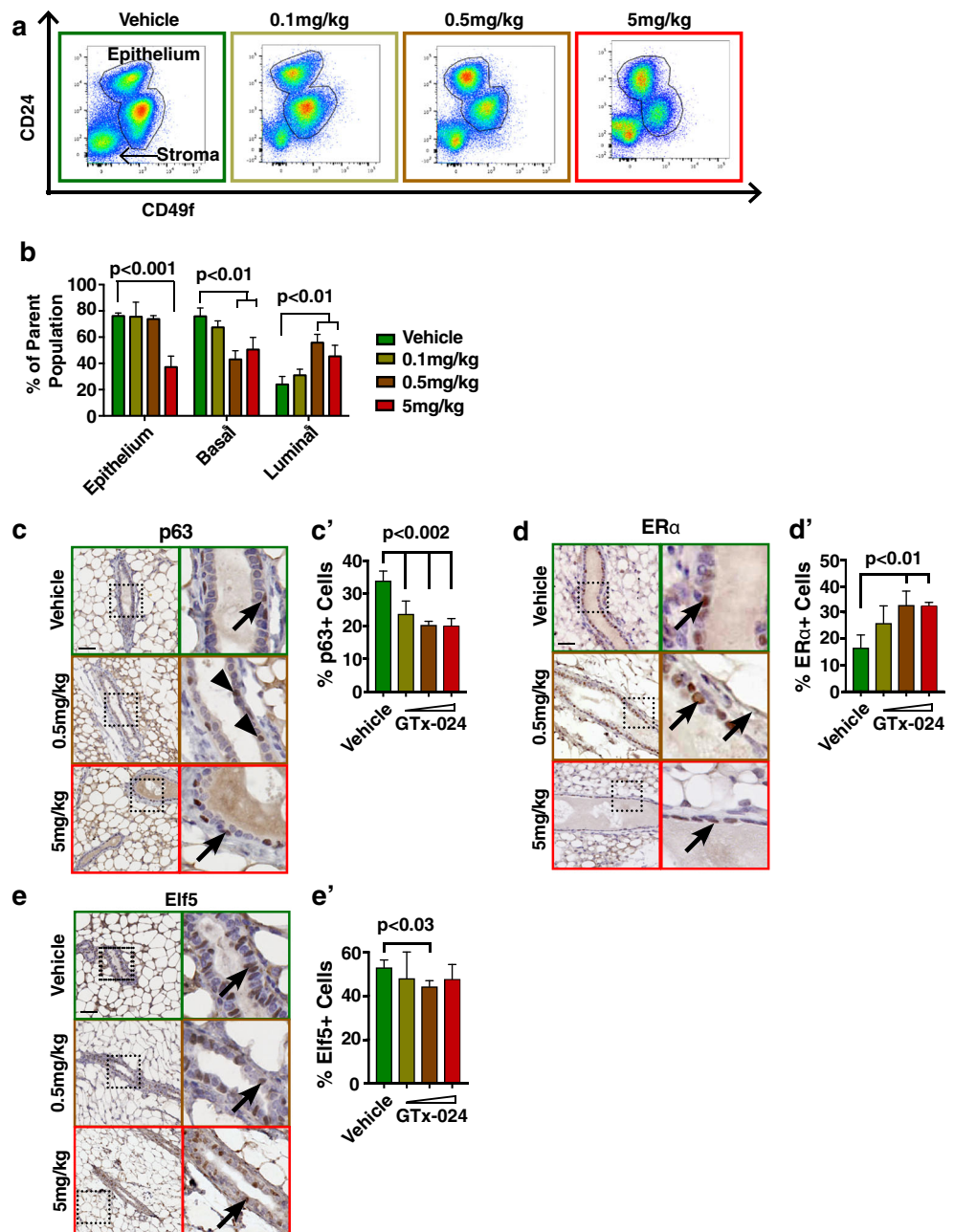
### AR is Expressed in Diverse Mouse MEC Populations and AR Ablation In Vivo Decreases the Proportion of Luminal MECs

To determine the principle target MEC population for AR action, immunohistological analysis of AR expression in vehicle- or GTx-024-treated mice was performed. The AR protein was expressed in a subset of basal and luminal MECs (Fig. 3A, arrowheads (basal MECs) & arrows (luminal MECs)) that is consistent with the potential for a direct response to androgens in both populations. (Examples of control staining on breast and prostate cancer tissue can be found in Supplemental Fig. S2A & S2B, respectively).

Despite the broad expression of AR amongst MEC sub-populations, AR-low/negative cells are apparent (Fig. 3A, asterisks). To support these findings, FACS-sorted basal, alveolar and HS-MEC populations were assessed by Fluidigm™ C1 to determine AR mRNA expression at a single cell level. All populations were found to harbour cells expressing AR mRNA, though basal and HS-MEC populations exhibited a higher proportion of AR-expressing MECs than did the alveolar population (Fig. 3B). This supports the possibility that AR directly functions in basal as well as HS-MECs. To functionally determine whether AR activity can modify MEC differentiation in vitro, FACS purified basal or luminal MECs were embedded in (basal) or layered atop (luminal) ECM gel and grown for 14 or 10 days, respectively, in the presence of the endogenous non-aromatisable AR agonist, DHT, alone or in combination with the AR antagonist, hydroxyflutamide. Hydroxyflutamide increased basal colony forming capacity, though this only reached near significance (Fig. 3C, with quantification in 3C',  $p = 0.052$ ), but did not modify luminal colony formation in the presence of DHT (Fig. 3D, with

**Fig. 2** AR activation alters the balance of mouse MEC lineages.

A) Representative flow cytometric plots of MECs from mice treated with vehicle or GTx-024, representing the proportion of stromal (CD24<sup>-</sup> and CD49f<sup>-</sup>) basal (CD24<sup>-</sup> and CD49f<sup>-</sup>) and luminal MECs (CD24<sup>+</sup> and CD49f<sup>-</sup>). B) Quantification of relative cellular proportions in mice from A. The proportion of luminal MECs increases at GTx-024 doses of 0.5 and 5 mg/kg/day ( $n = 5$  mice/group, mean  $\pm$  s.d.). C-E) Immunohistochemical staining of mammary gland tissue sections from vehicle- and GTx-024-treated mice (0.1, 0.5 and 5 mg/kg/day), probed for the basal marker p63 (C, with quantification in C', arrows show p63<sup>+</sup> MECs, arrowheads show p63<sup>+</sup> MECs with luminal position and morphology), luminal hormone-sensing cell marker, ER (arrows in D, with quantification in D'), and luminal alveolar marker Elf5 (arrows in E with quantification in E'). Note arrangement of p63-positive MEC in mice treated with 0.5 mg/kg GTx-024. ( $n = 5$  mice/group, graphed data plotted as mean  $\pm$  s.d., scale bars = 50  $\mu$ m)



quantification in D'). Such a modest effect of *in vitro* treatment may be explained by a loss of steroid receptor expression and activity through *in vitro* culture. To determine whether transgenic loss of AR activity could have the opposite effect on MEC populations *in vivo* compared to that observed for AR activation (Fig. 2C-D), the expression of p63 and ER was assessed in adult mice with global inactivation of the AR [10]. A significant increase in the proportion of p63-positive basal MECs (Fig. 2E, with quantification in E') and decrease in ER-positive luminal MECs (Fig. 2F, with quantification in F') was observed in AR-null mammary epithelium. Altogether these demonstrate that *in vivo* modulation of AR function alters the balance of MEC differentiation.

### AR is Expressed in a Subset of Basal Human MECs Present in Lobules Undergoing Developmental Transition

To assess the potential relevance of findings from the mouse to human breast, normal breast tissues harvested from reduction mammoplasties of pre-menopausal women were assessed for co-expression of AR with markers of MEC lineage specification by immunofluorescence. The highest AR-expressing cells were detected in lobular acini that possess relatively few MECs (Fig. 4Ai-ii, arrows versus arrowheads). In such lobules, cellular co-expression of AR with the basal marker p63 was observed (Fig. 4Aii, circles on magnified image in

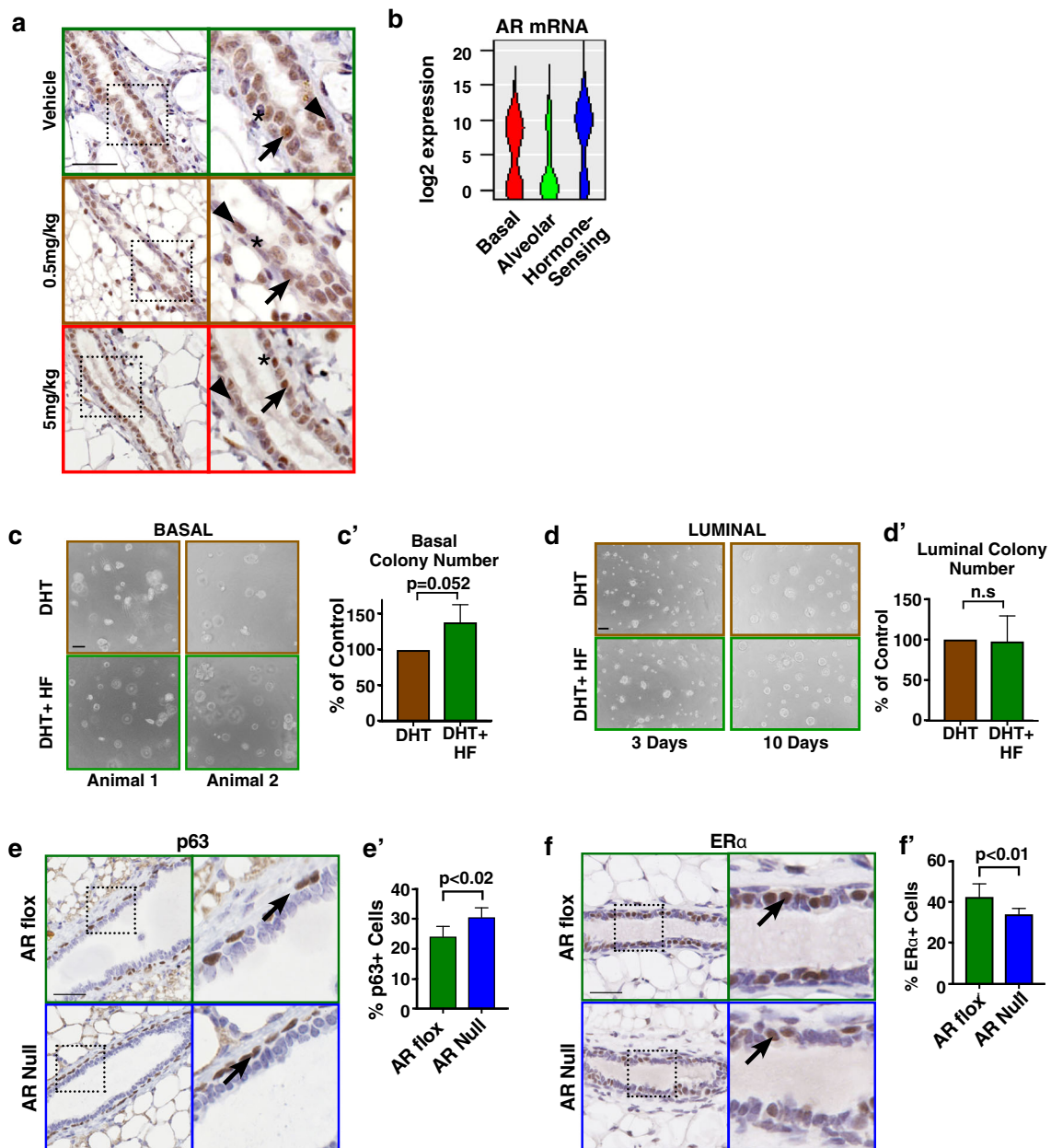


**Fig. 3** AR is expressed in diverse mouse MEC sub-populations and transgenic inactivation of AR alters the balance of mouse MEC lineages. **A**) Immunohistochemical staining of AR in vehicle- (green boxes) and GTx-024-treated (brown boxes – 0.5 mg/kg, red boxes – 5 mg/kg) mouse mammary tissue sections. Expression of AR is seen in multiple subsets of MECs (basal - arrowhead, luminal - arrows (positive), asterisks (low/negative), scale bar = 50  $\mu$ m, n = 5 animals/group). **B**) Violin plot of AR mRNA levels in FACS-sorted single basal, alveolar and HS-MECs (32 MECs/sub-population). **C**) Basal MECs isolated by FACS and embedded within ECM matrix gel and treated with dihydrotestosterone (DHT), or DHT in combination with the AR antagonist, hydroxyflutamide (HF). (n = 4 animals/group from 3

experiments, quantification of basal colony number in **C'** with data represented as a proportion of control (brown bar – DHT; green bar – DHT + HF). **D**) Luminal MECs from untreated mice FACS-isolated and cultured atop a layer of ECM gel and treated as in **C**. (n = 4 animals/group, quantification of colony number in **D'** with data represented as a proportion of control (brown bar – DHT, green bar – DHT + HF). **E-F**) Immunostaining in AR floxed (i.e. functional AR) and AR-null mouse mammary tissue sections, labeled for basal marker p63 (**E**, with quantification in **E'**) and luminal marker ER (**F**, with quantification in **F'**). n = 5 mice/group, graphed data plotted as mean  $\pm$  s.d, scale bar = 50  $\mu$ m)

“iii” denoted by dashed box in “ii”). Lobules containing AR- and p63-co-expressing MECs were rare (<1% of all MECs) but when identified possessed multiple co-expressing cells, suggesting developmental relevance (Fig. 4A and

Supplemental Fig. S3A-B). Of note, the highest AR-expressing MECs often existed in acini where p63-expressing basal MECs were sparse (4A, arrows), a result consistent with the idea that basal MECs may attain AR

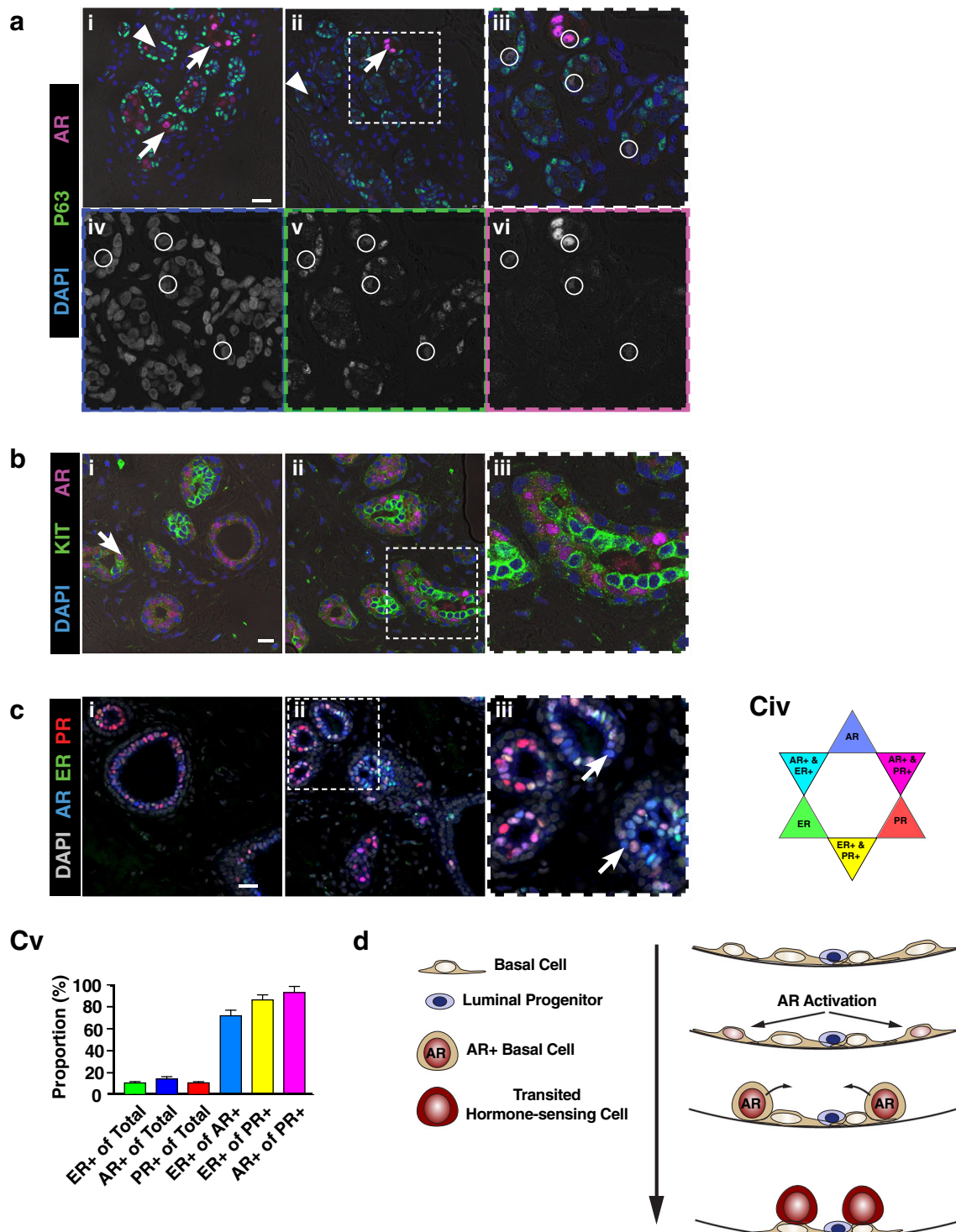


**Fig. 4** AR is expressed in a subset of basal human MECs. Immunofluorescence staining of human breast tissue sections derived from pre-menopausal reduction mammoplasties. **A)** Immunolabelling for the basal marker p63 (green), and the AR (magenta), and DAPI to detect nuclei (blue). A small proportion of MECs co-express AR and p63 (circles in magnified region “iii” denoted by dashed outline in “ii”) nuclei labeled with DAPI (grey). (scale bar = 25  $\mu$ m, representative staining from 12 samples). **A) iv-vi** - Individual channels from magnification in “iii” highlighting DAPI (iv), p63 (v) and AR (vi)-positive MECs (circles). **B)** Immunolabelling for the alveolar marker, KIT (green), the AR (magenta), and DAPI (blue). A small proportion of AR- and KIT-positive MECs are observed (i, arrowhead,  $3.3\% \pm 2.1\%$ ,  $n = 6$ ). **C)**

Triple immunofluorescence confocal microscopy of the AR (blue), ER (green) and PR (red) demonstrating AR-positive MECs that lack ER or PR expression (arrows in iii, (circles in magnified region “iii” denoted by dashed outline in “ii”) nuclei labeled with DAPI (grey). (scale bar = 25  $\mu$ m, representative staining from 12 samples). **Civ** = key to colors for marker colocalisation, Quantification of labeled cell proportions in **Cv**. (mean  $\pm$  s.d.). **D)** Proposed model for the role of AR in promoting a luminal phenotype in basal MECs, where expression of AR in basal MECs promotes population of the luminal niche and attainment of a luminal phenotype

expression as a part of a process of basal-to-luminal transition. This feature was observed only in isolated lobules of 3/12 assessed samples and therefore did not warrant quantification. Additional examples of p63 and AR co-expressing cells are shown in Supplemental Fig. S3. Expression of the luminal alveolar progenitor marker, KIT, was found to be highly distinct from AR expression in luminal MECs (Fig. 4Bi-ii, with magnification in “iii”), though a small proportion of AR-expressing MECs also expressed KIT (Fig. 4Bi - arrow, AR+ & cKIT+ = 3.3% ± 2.1%, *n* = 6), in line with the low expression of AR in the luminal alveolar sub-population of mouse MECs [16]. Analysis of AR localisation (Fig. 4C, blue) in combination with ER (Fig. 4C, green) and another HS-MEC marker, PR, (Fig. 4C, red, key for co-localisation of colors for triple staining shown in Fig. 4Civ) demonstrated that in human breast the bulk of AR expression was found within the luminal population and was co-expressed with ER and/or PR. Importantly, cells that express AR but lack ER or PR were readily observed, suggesting that AR more broadly regulates MECs beyond ER and/or PR-positive HS-MECs, consistent with results obtained from mouse experiments (Fig. 4C, arrows, and Supplemental Fig. S4, arrows, with quantification in Fig. 4Cv).

## Discussion

The presented data demonstrates that AR activation increases and AR inactivation decreases luminal cell identity in normal mouse MECs. The model within which we propose this occurs is conceptually illustrated in Fig. 4D. In this model, expression and activation of the AR in basal MECs promotes the attainment of luminal features (morphology, position and gene expression). This model is strongly supported by one study using FACS-sorted basal, alveolar and HS-MECs from mice, and analysed by microarray and network analysis using an in-house ROCK database [17]. In that study, of all genes presented as being enriched for a mammary lineage, AR was the only gene implicated in engaging both a basal and luminal gene network. When combined with the data presented herein, this supports the concept that the AR, and more broadly androgen signalling, can act in both basal and luminal MECs. In further support, the AR is a receptor shown to be enriched in breast cancer cells engrafted in the mammary gland through intraductal injection that maintains luminal profiles in cancer cells [18]. That study demonstrated that in the context of human breast cancer, AR signalling also promotes maintenance of a luminal state. Additional supportive data comes from AR lineage tracing studies in mouse prostate [19], which identified AR-expressing basal cells that are required for repopulation of the luminal niche after regression. Finally, a sub-population of ER-positive MECs was identified within

the basal population of mouse and human MECs [20, 21], which further supports the possibility of direct steroid responsiveness within the basal lineage.

Whether AR acts directly in mammary stem cells or a population of more differentiated basal progenitors is of interest in future studies. The Wnt-Notch axis greatly influences the balance of basal to luminal MECs, and maintenance of stem/basal MEC populations depends on functional Wnt signalling [22, 23]. An up-regulation in Wnt/β-Catenin signalling was observed in the mammary glands of transgenic mice lacking a functional AR [10], suggesting that the actions of AR activation observed in the present study could be derived from inhibition of the Wnt signalling pathway. In support of this notion, a similar reduction in the proportion of basal MECs and accumulation of ER-positive luminal MECs as observed in the present study, was reported in mice lacking the Wnt co-activator LBH [24].

A role for AR promoting luminal differentiation from basal MECs has a logical foundation in normal breast biology because the major female androgen, testosterone, act as the principle precursors to the most potent estrogenic compound in humans, 17β-estradiol [25]. Given the dependency of mammary function on estrogen signalling for pubertal mammary development [26–28] and to enable progestin responsiveness in adult MECs and human breast cancer cells [29–31], it is reasonable to speculate that AR activation is permissive to luminal function as it would serve as a signal that estrogenic precursors are sufficient to maintain the robust ER and PR signalling required for full mammary differentiation.

That AR functions in two distinct sub-populations of MECs – basal and HS-MECs – goes some way to explaining the divergent effect of clinical AR targeting in different breast cancer contexts (reviewed in [7]). Further delineating the molecular switches that drive these divergent functions of AR, and any cell subset-dependent actions, may provide a foundation from which to devise rational approaches to targeting the AR in different subtypes of breast cancer.

## Materials & Methods

### Mice & Tissue Harvesting

All animal experiments were performed in accordance with and approved by the University of Adelaide animal ethics committee (approval #M-2015-038). Normal 8 week-old inbred female FVB mice (University of Adelaide animal repository) were randomised to groups based on body weight and treated via drinking water with vehicle (2% Tween-20 in sterile H<sub>2</sub>O, Biorad #1706531) or 0.1, 0.5 or 5 mg/kg/day of the selective AR modulator, GTx-024 (Enobosarm - under materials transfer agreement with GTx, Memphis) for 16 weeks ± 5 days (depending on day of diestrus). Water bottles were

changed every 3 days. Estrus staging was performed daily, where relevant, as previously described [32]. Tissue from AR-null mice were harvested as previously described [10]. These mice were maintained at the ANZAC Research Institute. All procedures were approved by the Sydney Local Health District Animal Welfare Committee within NHMRC guidelines for animal experimentation.

### Human Tissue

Pre-menopausal human breast tissue was derived from reduction mammoplasties performed under informed consent at Flinders Medical Centre in adherence with the University of Adelaide Human Research Ethics Committee (approval#: H-2015-175).

### Carmine Staining Whole-Mounts

Mice were killed by exsanguination under deep anaesthesia and one number 3 (thoracic) gland was fixed, stained and processed as previously described [32]. Images were acquired with an Olympus SZX12 microscope.

### Isolation of Primary MECs, Cell Labelling, Flow-Cytometric Analysis, and Fluorescence-Activated Cell Sorting (FACS)

Mammary epithelial cells were isolated and fluorophore-conjugated antibody labelling was performed as previously described [33]. Cells were analyzed and sorted on a Becton-Dickinson FACS-Fusion containing 355 nm UV, 488 nm blue, 561 nm yellow-green, and 633 nm red lasers. Sorting for culture was performed into L15 (Sigma-Aldrich #L1518) with 6% FCS (Sigma-Aldrich #F2442). Gating hierarchy is outlined in Fig. S5.

### ECM-gel Basal and Luminal Colony-Formation Assays & Drug Treatments

A 50  $\mu$ L volume of phenol red-free and growth factor-reduced 100% ECM gel (Corning #356231) was added to a 48-well (luminal) or 96-well (basal) plate and allowed to solidify at 37 °C for 1 h. FACS-sorted basal MECs were re-suspended in growth media (20  $\mu$ L of DMEM/F12 (Sigma-Aldrich #D6434) supplemented with 5% charcoal-stripped FCS (Sigma-Aldrich #F2442) and 20 ng/mL murine epidermal growth factor (Sigma-Aldrich #E4127) and 1  $\times$  Penicillin-Streptomycin (Sigma #P4458)) at a concentration of 25,000 cells/mL and subsequently mixed with 80  $\mu$ L of ECM gel (Corning #356231). This mixture was layered over the solidified 100% ECM gel and allowed to solidify at 37 °C for a final cell concentration of 5000 cells/

well. FACS-sorted luminal MECs were re-suspended in growth media and layered over solidified ECM gel, without the addition of extra ECM gel, at a concentration of 10,000 cells/well and incubated at 37 °C for 10 days. Media was changed every 2 days. Treatment with dihydrotestosterone (DHT – Sigma-Aldrich #A8380) or hydroxyflutamide (Schering-Plough #16423) was performed for the duration of incubation. Drugs were reconstituted in 100% ethanol and diluted to a final concentration of 1 nM or 100 nM, respectively, in growth media. Colonies were quantified by taking low-magnification images of the entire well for each sample and treatment, and applying the “Find Edges” tool in Adobe Photoshop to demarcate individual colonies. Images were converted to binary format using ImageJ software (<https://imagej.nih.gov/ij/download.html>), after which the “Close” function was applied to complete colony circularity. The “Analyse Particles” function was used to quantify the number of colonies in each animal and treatment.

### Single Cell RNA Analysis

Mammary epithelial cells were isolated and fluorochrome-conjugated antibody labelling was performed as previously described [33]. A total of 96 cells were analyzed with 32 cells each for basal, luminal and HS-MEC subpopulations.

### Confocal Immunofluorescence

Immunofluorescence staining was performed as described elsewhere [32]. Antibodies employed are outlined in Supplemental Table S1. Images were sequentially acquired on a Leica SP5 spectral confocal microscope. Level adjustments were applied across entire images. Quantification of steroid receptor expression in primary breast tissue section was performed on 12 sections from the represented sample, by systematically sampling at 20 $\times$  magnification and selecting images based on the presence of epithelium (total cells counted = 2400). Briefly, Leica image format files were opened in ImageJ and segregated into individual channels. After converting to binary format, DAPI channels were used to define single cells, using the particle analysis tool, after which each channel was measured sequentially, and data exported to Microsoft Excel for analysis of proportions.

### Immunohistochemistry

Immunohistochemistry was performed as previously described [34]. Antibody dilutions were applied as outlined in Supplemental Table S1 and incubated overnight at 4 °C. Slides were scanned on a Nanozoomer slide scanner (Hamamatsu #C9600) and level adjustments applied

consistently to entire images. For quantification, entire scans were systematically sampled at 20× magnification and 8 images possessing mammary epithelium were acquired per sample. Every second image was manually quantified for marker-positive and -negative epithelial cells using ImageJ and the Cell Counter tool. A total of 600–800 cells were counted per animal per marker.

### Statistical Analysis

All data were analyzed by two-tailed t test or ANOVA with Tukey's multiple comparisons test. All data groups were verified for equality of variance by F test.

**Acknowledgements** The authors wish to acknowledge the support of the University of Adelaide Laboratory Animal Services, University of Adelaide Microscopy for imaging support, Dr. Randall Grose from the South Australian Health and Medical Research Institute for providing cell sorting services, Ms. Marie Pickering and Ms. Zoya Khityak for assistance with histological experiments, and Ms. Tamara Crittenden from Flinders Medical Centre for recruitment and consent of patients for primary breast tissue collection.

**Funding** This work was supported by funding from the National Breast Cancer Foundation (ID PS-15-041 to GAT and WDT), the National Health and Medical Research Council of Australia (ID APP1130077 and ID 1084416 to WDT and TEH), and Cancer Australia (ID 1043497). IMD is supported by a National Breast Cancer Foundation Fellowship ID PF-17-006. The laboratory of WDT & TEH is supported by research funds from GTx Inc., the manufacturers and suppliers of GTx-024 used in this study.

### Compliance with Ethical Standards

**Conflict of Interests** The authors declare no competing or financial interests.

**Independent Author Contributions** GAT: Devised concepts & hypotheses, performed experiments, interpreted data, devised conclusions, prepared manuscript. GLL: Performed experiments and analyzed data. MS: Performed single-cell RNA experiments and analyzed data. IMD: Assisted in performing mammary digestion and cell labelling. MMR: Assisted in performing mammary digestion and cell labelling. KAW & DJH: Design and development of AR null mice and supply of their mammary tissue. WDT: Reviewed data, manuscript preparation and editing. TEH: Experimental conceptual design, data revision, study supervision, manuscript editing.

### References

1. Briskin C, Duss S. Stem cells and the stem cell niche in the breast: an integrated hormonal and developmental perspective. *Stem Cell Rev.* 2007;3(2):147–56.
2. Rios AC, Fu NY, Lindeman GJ, Visvader JE. In situ identification of bipotent stem cells in the mammary gland. *Nature.* 2014;506(7488):322–7.
3. Van Keymeulen A, Rocha AS, Ousset M, Beck B, Bouvencourt G, Rock J, et al. Distinct stem cells contribute to mammary gland development and maintenance. *Nature.* 2011;479(7372):189–93.
4. Wuidart A, Ousset M, Rulands S, Simons BD, Van Keymeulen A, Blanpain C. Quantitative lineage tracing strategies to resolve multipotency in tissue-specific stem cells. *Genes Dev.* 2016;30(11):1261–77.
5. Colvin CW, Abdullatif H. Anatomy of female puberty: the clinical relevance of developmental changes in the reproductive system. *Clin Anat.* 2013;26:115–29.
6. Misiti S, Stigliano A, Borro M, Gentile G, Michienzi S, Cerquetti L, et al. Proteomic profiles in hyperandrogenic syndromes. *J Endocrinol Investig.* 2010;33(3):156–64.
7. Hickey TE, Robinson JLL, Carroll JS, Tilley WD. Minireview: the androgen receptor in breast tissues: growth inhibitor, tumor suppressor, oncogene? *Mol Endocrinol.* 2012;26(8):1252–67.
8. Tarulli GA, Butler LM, Tilley WD, Hickey TE. Bringing androgens up a NOTCH in breast cancer. *Endocr Relat Cancer.* 2014;4:T183–202.
9. Peters AA, Ingman WV, Tilley WD, Butler LM. Differential effects of exogenous androgen and an androgen receptor antagonist in the Peri- and Postpubertal murine mammary gland. *Endocrinology.* 2011;152(10):3728–37.
10. Gao YR, Walters KA, Desai R, Zhou H, Handelsman DJ, Simanainen U. Androgen receptor inactivation resulted in acceleration in pubertal mammary gland growth, upregulation of ER $\alpha$  expression, and Wnt/ $\beta$ -catenin signaling in female mice. *Endocrinology.* 2014;155(12):4951–63.
11. Barton VN, D'Amato NC, Gordon MA, Christenson JL, Elias A, Richer JK. Androgen receptor biology in triple negative breast Cancer: a case for classification as AR+ or quadruple negative disease. *Hormones Cancer.* 2015;6:206–13.
12. Dubois V, Simitsidellis I, Laurent MR, Jardi F, Saunders PT, Vanderschueren D, et al. Enobosarm (GTx-024) modulates adult skeletal muscle mass independently of the androgen receptor in the satellite cell lineage. *Endocrinology.* 2015;156(12):4522–33.
13. Barbareschi M, Pecciarini L, Cangi MG, Macri E, Rizzo A, Viale G, et al. p63, a p53 homologue, is a selective nuclear marker of myoepithelial cells of the human breast. *Am J Surg Pathol.* 2001;25(8):1054–60.
14. Yalcin-Ozuyal O, Fiche M, Guitierrez M, Wagner KU, Raffoul W, Briskin C. Antagonistic roles of Notch and p63 in controlling mammary epithelial cell fates. *Cell Death Differ.* 2010;17(10):1600–12.
15. Oakes SR, Naylor MJ, Asselin-Labat ML, Blazek KD, Gardiner-Garden M, Hilton HN, et al. The Ets transcription factor E1f5 specifies mammary alveolar cell fate. *Genes Dev.* 2008;22(5):581–6.
16. Regan JL, Kendrick H, Magnay F-A, Vafaizadeh V, Groner B, Smalley MJ. C-kit is required for growth and survival of the cells of origin of Brca1-mutation-associated breast cancer. *Oncogene.* 2012;31(7):869–83.
17. Kendrick H, Regan JL, Magnay F-A, Grigoriadis A, Mitsopoulos C, Zvelebil M, et al. Transcriptome analysis of mammary epithelial subpopulations identifies novel determinants of lineage commitment and cell fate. *BMC Genomics.* 2008;9(1):591.
18. Sflomos G, Dormoy V, Metsalu T, Jeitzner R, Battista L, Scabia V, et al. A preclinical model for ER $\alpha$ -positive breast Cancer points to the epithelial microenvironment as determinant of luminal phenotype and hormone response. *Cancer Cell.* 2016;29(3):407–22.
19. Xie Q, Liu Y, Cai T, Horton C, Stefanson J, Wang ZA. Dissecting cell-type-specific roles of androgen receptor in prostate homeostasis and regeneration through lineage tracing. *Nat Commun.* 2017;8:14284.
20. Dall GV, Vieusseux JL, Korach KS, Arao Y, Hewitt SC, Hamilton KJ, et al. SCA-1 labels a subset of estrogen-responsive Bipotential repopulating cells within the CD24+ CD49fhi mammary stem cell-enriched compartment. *Stem Cell Rep.* 2017;8(2):417–31.
21. Hilton HN, Graham JD, Kantimm S, Santucci N, Cloosterman D, Huschtscha LI, et al. Progesterone and estrogen receptors segregate

- into different cell subpopulations in the normal human breast. *Mol Cell Endocrinol.* 2012;361(1–2):191–201.
22. van Amerongen R, Bowman AN, Nusse R. Developmental stage and time dictate the fate of Wnt/ $\beta$ -catenin-responsive stem cells in the mammary gland. *Cell Stem Cell.* 2012;11(3):387–400.
  23. Zeng YA, Nusse R. Wnt proteins are self-renewal factors for mammary stem cells and promote their long-term expansion in culture. *Cell Stem Cell.* 2012;6(6):568–77.
  24. Lindley LE, Curtis KM, Sanchez-Mejias A, Rieger ME, Robbins DJ, Briegel KJ. The WNT-controlled transcriptional regulator LBH is required for mammary stem cell expansion and maintenance of the basal lineage. *Development.* 2015;142(5):893–904.
  25. Blakemore J, Naftolin F. Aromatase: contributions to physiology and disease in women and men. *Physiology.* 2016;31(4):258–69.
  26. Bocchinfuso WP, Lindzey JK, Hewitt SC, Clark JA, Myers PH, Cooper R, et al. Induction of mammary gland development in estrogen receptor-alpha knockout mice. *Endocrinology.* 2000;141(8):2982–94.
  27. Ciarloni L, Mallepell S, Brisken C. Amphiregulin is an essential mediator of estrogen receptor alpha function in mammary gland development. *Proc Natl Acad Sci U S A.* 2007;104(13):5455–60.
  28. Cunha GR, Young P, Hom YK, Cooke PS, Taylor JA, Lubahn DB. Elucidation of a role for stromal steroid hormone receptors in mammary gland growth and development using tissue recombinants. *J Mammary Gland Biol Neoplasia.* 1997;2(4):393–402.
  29. Katzenellenbogen BS, Norman MJ. Multihormonal regulation of the progesterone receptor in mcf-7 human breast cancer cells: interrelationships among insulin/insulin-like growth factor-i, serum, and estrogen. *Endocrinology.* 1990;126(2):891–8.
  30. Lain AR, Creighton CJ, Conneely OM. Research resource: progesterone receptor targetome underlying mammary gland branching morphogenesis. *Mol Endocrinol.* 2013;27(10):1743–61.
  31. Petz LN, Ziegler YS, Schultz JR, Kim H, Kemper JK, Nardulli AM. Differential regulation of the human progesterone receptor gene through an estrogen response element half site and Sp1 sites. *J Steroid Biochem Mol Biol.* 2004;88(2):113–22.
  32. Tarulli GA, De Silva D, Ho V, Kunasegaran K, Ghosh K, Tan BC, et al. Hormone-sensing cells require Wip1 for paracrine stimulation in normal and premalignant mammary epithelium. *Breast Cancer Res: BCR.* 2013;15(1):R10.
  33. Shehata M, Teschendorff A, Sharp G, Novcic N, Russell IA, Avril S, et al. Phenotypic and functional characterisation of the luminal cell hierarchy of the mammary gland. *Breast Cancer Res.* 2012;14(5):R134.
  34. Mohammed H, Russell IA, Stark R, Rueda OM, Hickey TE, Tarulli GA, et al. Progesterone receptor modulates ER $\alpha$  action in breast cancer. *Nature.* 2015;523(7560):313–7.